

Original Research

New Green Chemistry Approach of Synthesis of Aryl Substituted Dihydro Pyrimidone Derivatives Using Citrus Extract for Antibacterial and Antifungal Activities

Ghaferah H. Al-Hazmi*

Department of Chemistry, College of Science, Princess Nourah bint Abdulrahman University,
P.O. Box 84428, Riyadh 11671, Saudi Arabia

Received: 1 December 2023

Accepted: 8 February 2024

Abstract

This study utilizes a novel green chemistry method to synthesize aryl-substituted dihydropyrimidone derivatives (P1-P7), with structural information determined through various analytical techniques, including IR, ¹H-NMR, HPLC, GCMS, and CHNS elemental analysis. The photophysical properties of the synthesized molecules were assessed using the DFT-B3LYP-6-31G(d) basis set within the Gaussian-09w software. The molecule P1 shows the highest bandgap of 4.497eV. The GCRD parameters reveal the high electrophilic behavior of P4 and P5. The general findings derived from the GCRD parameter indicate that the synthesized molecules exhibit a pronounced reactivity. Furthermore, the synthesized molecules were evaluated for antibacterial and antifungal activities, demonstrating that P4 and P5 exhibit heightened reactivity against *S. typhi*, *E. coli*, *A. niger*, and *C. albicans*.

Keywords: dihydro pyrimidone derivatives, DFT, HOMO-LUMO, biological activity

Introduction

In the vast canvas of organic chemistry, the allure of pyrimidone derivatives beckons researchers with the promise of unlocking new frontiers in biological applications. This class of compounds, distinguished by the presence of the pyrimidine nucleus, a cornerstone in medicinal chemistry, stands as a crucial pharmacophore, with the synthesis of novel derivatives emerging

as a focal point in contemporary drug discovery [1-3]. This dynamic pursuit is not merely a scientific endeavor but an artistic exploration into the realms of potential therapeutic advancements. Within the intricate molecular design, the synthesis of innovative pyrimidine derivatives takes center stage, captivating the imagination of researchers as they endeavor to craft compounds that transcend the ordinary.

Biginelli adducts have demonstrated notable biological properties encompassing calcium channel inhibition, antioxidant, antiviral, antimicrobial, antitubercular, and anti-inflammatory activities [4-7]. The therapeutic potential of dihydropyrimidinones

*e-mail: dr.ghaferah@yahoo.com

has prompted the exploration of modified techniques for the Biginelli reaction. The initial approach involves a one-pot, multicomponent reaction involving benzaldehyde, ethyl acetoacetate, and urea in ethanol under reflux conditions with the presence of HCl, yielding the desired Biginelli adduct. Although several methodologies have been developed in recent years, many suffer from limitations such as harsh conditions, extended reaction times, low yields, and the use of expensive catalysts, making them less compatible with green chemistry principles [8-11].

An essential focus in recent catalysis research revolves around green reaction media [12, 13]. Metal oxide nanoparticles have demonstrated the ability to catalyze various organic transformations on their active surfaces and interstitial cavities [14, 15]. PEG-400 has emerged as a green, benign, and recyclable solvent, serving both as a solvent and catalyst for numerous reactions [16, 17]. Ongoing efforts are dedicated to devising methods for the synthesis of diverse organic compounds [18, 19]. The utilization of ultrasound and microwave methods is noteworthy for their safety and efficiency in terms of reaction time [20, 21]. In view of the above, in the present work, aryl substituted dihydro pyrimidone was synthesized using the green synthesis method and is estimated to have photophysical and biological applications.

Materials and Methods

The urea, thiourea, N-methyl urea, anisaldehyde, salicylaldehyde, p-chlorobenzaldehyde, p-nitrobenzaldehyde and p-fluorobenzaldehyde were sourced from Spectro Chem and employed following the manufacturer instructions. The chemical reactions were conducted under standard atmospheric conditions. Thin-layer chromatography plates composed of silica gel were used, and ethyl acetate in hexane served as the mobile phase for monitoring the reaction. Melting points were determined using open capillaries and a melting point apparatus. Tetramethyl silane (TMS) was used as an internal reference for $^1\text{H-NMR}$ spectra, which were acquired using a Jeol (400 MHz) nuclear magnetic resonance spectrometer with $\text{DMSO-}d_6$ as the solvent. Chemical shift values are reported in delta (parts per

million, ppm). HPLC and mass analysis of the resulting compounds were performed using a 1290 Infinite UHPLC instrument. The synthesized compounds' infrared spectra ($4000\text{-}350\text{ cm}^{-1}$) were captured in KBr pellets using a Bruker IR spectrophotometer.

Synthesis of the Aryl Substituted Dihydro Pyrimidone Derivative

The aryl substituted dihydro pyrimidone derivative was synthesized using the one pot synthesis method (Fig. 1). Initially, a combination of aromatic aldehydes (20 mmol), along with urea/thiourea/methyl urea (20 mmol) and ethyl acetoacetate (20 mmol), was subjected to reflux in ethanol in the presence of a catalytic amount of concentrated hydrochloric acid for 2 hours. Following confirmation of reaction completion through thin-layer chromatography, the reaction mixture was cooled and introduced to crushed ice water. The resulting solid product was filtered and washed with water, and the crude product underwent recrystallization with ethanol. Further, the identical derivative was produced using an environmentally friendly synthesis method. Initially, both grapefruit (*Citrus maxima*) and dessert lime (*Citrus medica*) underwent thorough washing and were subsequently dried by patting. Afterward, the fruits were halved. The extraction process involved using a citrus juice squeezer for the dessert lime and gently pressing the grapefruit halves with a pestle and mortar. The grapefruit juice was then filtered through cotton to obtain a clear solution. For the synthesis, separate round-bottom flasks were used to contain 20 mmol of aromatic aldehydes, 20 mmol of ethyl acetoacetate, and 20 mmol of urea. Natural catalysts (*Citrus maxima* or *Citrus medica*) were introduced by adding 10 mL of grapefruit juice to one flask and dessert lime juice to the other. The mixtures were stirred at room temperature for 10 to 12 hours, with TLC used to monitor the reaction's progress. Upon completion, the reaction mixtures were filtered and washed with water, and the resulting solid product underwent recrystallization with ethanol. All synthesized compounds were subsequently confirmed through FTIR, $^1\text{H-NMR}$, and mass spectroscopy and are given in Fig. S1-28.

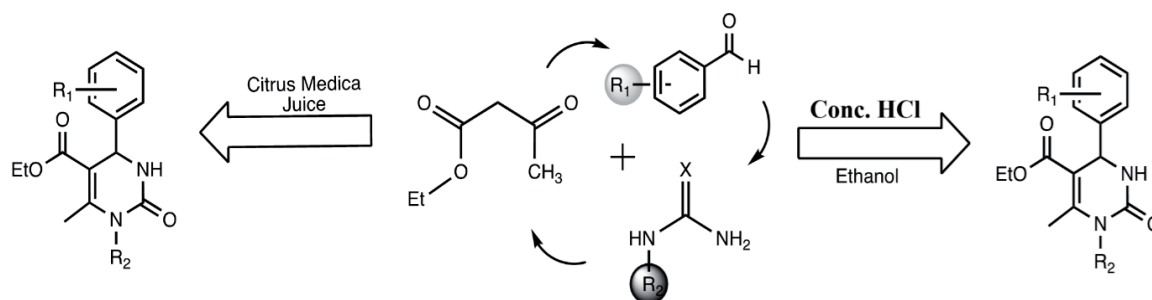


Fig. 1. Synthesis of the aryl substituted dihydro pyrimidone.

Structural Data of Aryl Substituted
Dihydro Pyrimidone.

Ethyl-6-methyl-2-oxo-4-phenyl-1,2,3,4-tetrahydropyrimidine-5-carboxylate (P1)

Melting point: 198°C, Percentage yield: 84%. ¹H-NMR (DMSO-*d*₆, 400 MHz): δ ppm 9.2 (s, 1H), 7.7 (m, 1H), 7.2-7.4 (m, 5H), 5.1 (s, 1H), 3.9 (q, 3H), 2.2 (s, 3H), 1.1 (t, 3H). High Resolution MS: *m/z* 261.12. HPLC purity was found to be: 91.70 %. IR (KBr, cm⁻¹): 3200-3100 (N-H stretching), 1750-1700 (C=O of ester), 1650 (C=O of amide).

Ethyl-4-(4-chlorophenyl)-6-methyl-2-oxo-1,2,3,4-tetrahydropyrimidine-5-carboxylate (P2)

Melting point: 224°C, Percentage yield: 80%. ¹H-NMR (DMSO-*d*₆, 400 MHz): δ ppm 9.2 (s, 1H), 7.8 (m, 1H), 7.4 (m, 2H), 7.2 (m, 2H), 5.1 (s, 1H), 3.9 (q, 3H), 2.2 (s, 3H), 1.1 (t, 3H). High Resolution MS: The mass of the compound was found to be 295.28 g/mol. HPLC purity was found to be 92.66%. IR (KBr, cm⁻¹) 3200-3100 (N-H stretching), 1750-1700 (C=O of ester), 1650 (C=O of amide).

Ethyl 4-(4-fluorophenyl)-6-methyl-2-oxo-1,2,3,4-tetrahydropyrimidine-5-carboxylate (P3)

Melting point: 164°C, Percentage yield: 84%, ¹H NMR (DMSO-*d*₆, 400 MHz): δ ppm 9.2 (s, 1H), 7.8 (s, 1H), 7.3 (m, 2H), 7.1 (m, 2H), 4.0 (q, 3H), 2.2 (s, 3H), 1.1 (t, 3H), 5.1 (s, 1H), High Resolution MS: The mass of the compound was found to be 279.11 g/mol HPLC purity was found to be 97.99 %. IR (KBr, cm⁻¹) 2918, 2825, 1597, 1387, and 483.

Ethyl-4-(4-methoxyphenyl)-6-methyl-2-oxo-1,2,3,4-tetrahydropyrimidine-5-carboxylate (P4)

Melting point: 188°C, Percentage yield: 83%, ¹H-NMR (DMSO-*d*₆, 400MHz): δ ppm 9.2 (s, 1H), 7.7 (m, 1H), 7.1 (m, 2H), 6.8 (m, 2H), 5.1 (m, 1H), 3.9 (q, 2H), 3.8 (s, 3H), 2.2 (s, 3H), 1.1 (t, 3H) High Resolution MS: The mass of the compound was found to be 291.13 g/mol, HPLC purity was found to be 94.63 %. IR (KBr, cm⁻¹) 2936, 2832, 1677, 1605, and 1237.

Ethyl-4-(2-hydroxyphenyl)-6-methyl-2-oxo-1,2,3,4-tetrahydropyrimidine-5-carboxylate (P5)

Melting point: 190°C, Percentage yield: 82%, ¹H-NMR (DMSO-*d*₆, 400MHz): δ ppm 9.6 (s, 1H), 9.1 (s, 1H), 7.1-7.4 (m, 4H), 5.4 (s, 1H), 4.1 (q, 1H), 3.9 (q, 2H), 2.2 (s, 3H), 1.0 (t, 3H) High Resolution MS: The mass of the compound was found to be 276.11 g/mol. HPLC purity was found to be 89.98%. IR (KBr, cm⁻¹) 3440, 3119, 2993, 1689, 1593, and 1117.

Ethyl-6-methyl-4-phenyl-2-sulfanylidene-1,2,3,4-tetrahydropyrimidine-5-carboxylate (P6)

Melting point: 170°C, Percentage yield: 92%, ¹H-NMR (DMSO-*d*₆, 400MHz): δ ppm 10.3 (s, 1H), 9.6 (s, 1H), 7.3 (m, 5H), 5.1 (s, 1H), 4.0 (m, 2H), 2.2 (s, 3H), 1.1 (t, 3H). High Resolution MS: The mass of the compound was found to be 277.10g/mol. HPLC purity was found to be 83.9 %. IR (KBr, cm⁻¹) 2975, 2832, 1592, and 1371.

Ethyl-1,6-dimethyl-2-oxo-4-phenyl-1,2,3,4-tetrahydropyrimidine-5-carboxylate (P7)

Melting point: 168°C, Percentage yield: 90%, ¹H-NMR (DMSO-*d*₆, 400MHz): δ ppm 8.0 (s, 1H), 7.3 (m, 2H), 7.2 (m, 3H), 5.1 (s, 1H), 4.0 (m, 2H), 3.1 (s, 3H), 2.5 (s, 3H), 1.1 (t, 3H). High Resolution MS: The mass of the compound was found to be 275.13g/mol, HPLC purity was found to be 95.25%. IR (KBr, cm⁻¹) 2971, 2822, 2722, 1577 and 1333.

Results and Discussion

The molecular structure and reactant used for the reaction are given in Table 1. The molecular structure of the ¹H-NMR spectra of derivatives P1-P7 was recorded in DMSO-*d*₆, as depicted in Fig. S1-7. In P1, a sharp singlet at δ: 2.2 ppm indicated the presence of a methyl substituent attached to a pyrimidine ring. Methylene (-CH₂-) and methyl (-CH₃-) groups linked with oxygen [-O(CH₂CH₃)] resonated at δ: 3.9 ppm and δ: 1.1 ppm, respectively, as a quartet and triplet. Singlets at δ: 5.1 and 9.2 ppm provided insight into the -NH protons in the pyrimidine architecture, while aromatic protons resonated as a multiplet in the range δ: 7.2-7.4 ppm. In molecule P2, a singlet peak at δ: 2.2 ppm corresponded to free methyl, and singlets at δ: 9.2 ppm and δ: 7.3 ppm were attributed to the -NH moiety in the six-membered heterocyclic ring. Methylene and methyl protons in [-O(CH₂CH₃)] resonated at δ: 4.0 and δ: 1.1 ppm as a quartet and triplet, respectively. Aromatic peaks in the range δ: 7.1 to 7.3 ppm appeared as multiplets. Molecule P3 exhibited sharp singlets at δ: 2.23 ppm, δ: 9.2 ppm, and δ: 7.3 ppm for free methyl and two -NH moieties attached to the six-membered heterocyclic pyrimidine architecture, respectively. The ethyl moiety in [-O(CH₂CH₃)] resonated as a quartet and triplet at δ: 4.0 and δ: 1.1 ppm. Aromatic protons displayed multiplets in the range δ: 7.1 to 7.3 ppm. In molecule P4, two -NH protons resonated as singlets at δ: 9.2 ppm and δ: 7.1 ppm, while methyl groups resonated at δ: 2.2 ppm and δ: 3.8 ppm as a singlet, indicating methyl and methoxy substitution. Methylene and methyl groups [-O(CH₂CH₃)] resonated at δ: 3.9 ppm and δ: 1.1 ppm, respectively. Aromatic protons appeared as a multiplet in the range δ: 6.8-7.1 ppm. Derivative P5 displayed singlets at δ: 9.6 ppm, δ: 9.1 ppm, and δ: 2.2 ppm for two

-NH and a methyl substitution, respectively. Methylene and methyl groups [-O(CH₂CH₃)] resonated as a quartet and triplet at δ :3.9 and δ :1.0 ppm. Aromatic protons in the region δ :7.1-7.4 ppm indicated their presence as a multiplet. P6 exhibited singlets at δ :10.3, δ :9.6, and 2.2 ppm for two -NH and a free methyl group. Quartet and triplet peaks at δ :4.0 and δ :1.1 ppm corresponded to methylene and methyl groups [-O(CH₂CH₃)], and aromatic protons resonated in the range δ :7.1-7.3 ppm as a multiplet. Molecule P7 showed singlets at δ :8.0 ppm, δ :3.1 ppm, and δ :2.5 ppm for -NH, -NCH₃, and free methyl groups, respectively. Methylene and methyl groups [-O(CH₂CH₃)] resonated as a quartet and triplet at δ :4.0 and δ :1.1 ppm. Aromatic protons were multiplets in the region δ :7.2-7.3 ppm. Additionally, all synthesized derivatives exhibited a junction -CH at δ :5.1 ppm - 5.4 ppm as a singlet. The FT-IR spectra of the synthesized mono-azo derivatives revealed valuable information about the functional groups, explaining the characteristics of stretching modes of vibration for the azo molecules. HPLC and mass analysis of the resulting compounds P1-P7 were investigated and assigned (Fig. S8-22). Fig. S23-28 depicts the FT-IR spectra, with bands at 3246 cm⁻¹ indicating the presence of -NH groups. Another band at 1726 cm⁻¹ was attributed to the -C=O functional group in the cyclic ring moiety, and -C-O functionality was displayed at 1117 cm⁻¹. The synthesized derivatives displayed aromatic -CH stretching bands in the region 3100-2800 cm⁻¹, and 1670-1650 cm⁻¹ were related to -CONH groups. Aromatic substituted halides showed Ar-X in the range of 1000-500 cm⁻¹.

Computational Photo Physical Studies

In this study, Gaussian 16 software was employed for a comprehensive computational investigation into the synthesized molecules. The optimization of ground-state geometry was meticulously conducted using the DFT-B3LYP-6-31G(d) basis set. The resulting HOMO-LUMO energy levels, derived from the optimized geometry, were quantified and meticulously recorded in Table 1. The calculated HOMO and LUMO values, expressed in electron volts (eV), facilitated a thorough assessment of the band gap for the synthesized compounds, as systematically presented in Table 2.

Remarkably, the designed compounds (denoted as P1 to P7) featuring distinct positional groups displayed a narrowed energy gap when compared to molecule P5. The latter, characterized by a highly electronegative bromobenzene attached to the main moiety, underscored the substantial influence of functional group types on the energy gap of the molecules. Specifically, molecule P5 exhibited the smallest energy band gap, attributed to the presence of the phenol unit, as meticulously outlined in Table 2. The ranking of the energy band gap for all examined molecules unfolded as follows: P1>P4>P7>P3>P2>P6>P5. Overall, the theoretically predicted molecules demonstrated an enhanced

capacity for charge transfer between molecular orbitals, thereby indicating their potential suitability for diverse biological applications [22, 23].

To gain a deeper understanding of the molecular orbitals (MOs) in the designed molecules, an assessment of the distribution of frontier molecular orbitals (FMOs) was undertaken. Detailed contour plots of the frontier orbitals HOMO and LUMO for the molecular systems are thoughtfully presented in Table 2. The density of HOMO and LUMO elegantly spans across the 6-methyl-4-phenyl-3,4-dihydropyrimidin-2(1H)-one group. The perfect superposition of these diminutive donor candidates highlights their intriguing properties for facilitating electron transport from the HOMO to the LUMO orbital.

In our quest for insights into the chemical reactivity and stability of the synthesized molecules, global reactivity parameters were calculated. These global reactivity descriptor (GCRD) parameters encompass chemical hardness (η), electronegativity (χ), chemical potential (μ), chemical softness (S), and electrophilicity index (ω) and the equation involved in the GCRD parameter is given supplementary information. The ionization potential (IP) and electron affinity (EA) were pivotal in these calculations. The resulting global reactivity parameters are meticulously detailed in Table 3.

$$\text{Chemical hardness } (\eta = (IP - EA)/2)$$

$$\text{Electronegativity } (\chi = (IP + EA)/2)$$

$$\text{Chemical potential } (\mu = -\chi)$$

$$\text{Chemical softness } (S = 1/2\eta)$$

$$\text{Electrophilicity index } (\omega = \mu^2/2\eta)$$

$$\text{Ionization potential, } IP = -E_{HOMO}$$

$$\text{Electron affinity, } EA = -E_{LUMO}$$

A lower ionization potential (IP) coupled with a higher electron affinity (EA) signals a robust electron transport capability. From the findings presented in Table 2, the ionization potential (IP) values traverse a range from 6.110 eV to 5.646 eV in the following order: P6>P2>P3>P1>P4>P7>P5. Compound P7 emerges with a lower IP value, indicating its relatively diminished electron donor capability among the studied compounds. Meanwhile, the electron affinity (EA) values, spanning from 1.238 eV to 1.743 eV, showcase P6 with the maximum EA value, underscoring its superior electron transport capability. The pursuit of enhanced charge transfer and separation emphasizes the significance of a small chemical hardness (η) value. Notably, from Table 2, molecule P5 stands out with the lowest chemical hardness among the studied molecules.

Table 1. List of the aryl substituted dihydro pyrimidone.

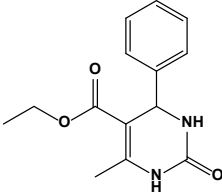
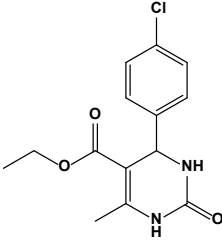
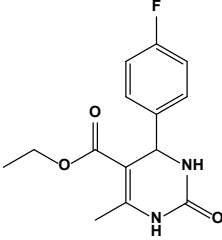
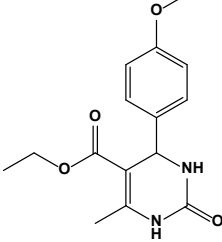
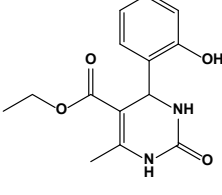
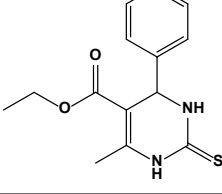
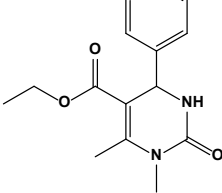
Compound	Aldehyde R ₁	X/R ₂	Product	Yield
P1	H	O/H		84%.
P2	4-Cl	O/H		80%
P3	4-F	O/H		84 %
P4	4-OCH ₃	O/H		83%
P5	2-OH	O/H		82 %
P6	H	S/H		92 %
P7	H	O/CH ₃		90 %

Table 2. GCRD parameters obtained from HOMO-LUMO and dipole moment of newly synthesized compounds (P1-P7).

Sample	E_{HOMO} (eV)	E_{LUMO} (eV)	ΔE (eV)	IP (eV)	EA (eV)	η (eV)	χ (eV)	μ (eV)	S (eV ⁻¹)	ω (eV)
P1	-5.831	-1.334	4.497	5.831	1.334	2.248	3.583	-3.583	0.222	2.855
P2	-5.974	-1.574	4.400	5.974	1.575	2.200	3.775	-3.775	0.227	3.238
P3	-5.942	-1.507	4.435	5.942	1.508	2.218	3.725	-3.725	0.225	3.129
P4	-5.706	-1.245	4.461	5.706	1.246	2.230	3.476	-3.476	0.224	2.709
P5	-5.646	-1.426	4.219	5.646	1.427	2.110	3.536	-3.536	0.237	2.964
P6	-6.110	-1.743	4.367	6.110	1.743	2.184	3.927	-3.927	0.229	3.531
P7	-5.678	-1.237	4.441	5.678	1.238	2.220	3.458	-3.458	0.225	2.693

Further exploration into the stabilization energies of the molecular structures, measured by the electrophilicity index (ω), reveals that the designed molecule P6 exhibits the highest electron-accepting power and stabilization energy among its counterparts, an attribute attributed to the presence of chlorobenzene [24]. This comprehensive analysis sheds light on the intricate molecular landscape and paves the way for further exploration of these compounds in diverse applications.

In vitro Antimicrobial and Antifungal Activity

We conducted antimicrobial and antifungal studies on the recently synthesized molecules, denoted as (P1-P7). Significantly, compounds P4 and P5 displayed notable antibacterial efficacy against *S. aureus*, *B. subtilis*, *S. typhi*, *E. coli*, *A. niger*, and *C. Albicans*. The heightened activity of these compounds is likely attributed to the presence of biologically active anisole and phenol groups attached to the pyrimidone in P4 and P5. Fluorine, being the second-smallest substituent, shares similarities with hydrogen in terms of steric

requirements at enzyme receptor sites. The incorporation of fluorine has been shown to enhance absorption rates by increasing lipid solubility [25]. The highly lipophilic nature of the trifluoromethyl group plays a significant role in improving pharmacological activity. Conversely, the remaining molecules exhibited minimal antibacterial activity [26]. Detailed data for all other molecules with moderate antibacterial activity are presented in Table 3. All other compounds demonstrated moderate activity; data and minimum inhibitory concentrations (MIC) are provided in Table 3's parenthesis.

Conclusions

In summary, we have successfully demonstrated a convenient green chemistry method for synthesizing a diverse range of aryl-substituted dihydropyrimidone derivatives (P1-P7). The synthesized compounds were characterized using spectral and analytical methods. HOMO-LUMO energy levels were estimated through the DFT-B3LYP-6-31G(d) basis set within the Gaussian-

Table 3. Antimicrobial and antifungal activity of the aryl substituted dihydro pyrimidone derivatives.

Compounds	<i>S. aureus</i>	<i>B. subtilis</i>	<i>S. typhi</i>	<i>E. coli</i>	<i>A. niger</i>	<i>C. albicans</i>
P1	19	20	18	17	20	21
P2	21	23	19	20	21	18
P3	21	24	22	24	23	21
P4	21	26	21	26	26	27
P5	22	27	26	27	27	25
P6	20	22	21	22	18	22
P7	23	21	22	19	21	24
Standard ^a	25	25	23	25	23	24
Control ^b DMSO	0	0	0	0	0	0

Note: ^aStandard drugs employed were Ciprofloxacin (40 μg in 100 μL) for bacteria and Fluconazole (40 μg in 100 μL) for fungi. The tested compounds were utilized at concentrations of 40 μg in 100 μL , and the corresponding measurements of zone of inhibition were expressed in millimetres, ^bControl: DMSO (Dimethyl sulphoxide).

09W software. GCRD parameters were derived from the theoretically estimated HOMO-LUMO energy levels, revealing that P4 and P5 exhibit highly electrophilic behavior. Moreover, the antibacterial and antifungal activities of the synthesized molecules were assessed against *S. aureus*, *B. subtilis*, *S. typhi*, *E. coli*, *A. niger*, and *C. albicans*. The biological application results indicate that P4 and P5 molecules exhibit potent antibacterial and antifungal behavior.

Acknowledgments

Princess Nourah bint Abdulrahman University Researchers Supporting Project number (PNURSP2024R76), Princess Nourah bint Abdulrahman University, Riyadh, Saudi Arabia.

Conflict of Interests

The authors declare no conflict of interests.

References

- ZHANG Y., PIKE A. Pyridones in drug discovery: recent advances. *Bioorganic & Medicinal Chemistry Letters*, **38**, 127849, **2021**.
- ZHUANG J., MA S. Recent development of pyrimidine-containing antimicrobial agents. *ChemMedChem*, **15** (20), 1875, **2020**.
- PATEL R.V., KEUM Y.S., PARK S.W. Sketching the historical development of pyrimidones as the inhibitors of the HIV integrase. *European Journal of Medicinal Chemistry*, **97**, 649, **2015**.
- DE FÁTIMA Â., BRAGA T.C., NETO L.D.S., TERRA B.S., OLIVEIRA B.G., DA SILVA D.L., MODOLO L.V. A mini-review on Biginelli adducts with notable pharmacological properties. *Journal of Advanced Research*, **6** (3), 363, **2015**.
- MARINESCU M. Biginelli reaction mediated synthesis of antimicrobial pyrimidine derivatives and their therapeutic properties. *Molecules*, **26** (19), 6022, **2021**.
- DE FÁTIMA A., TERRA B.S., SILVA-NETO L., BRAGA T.C. Organocatalyzed Biginelli reactions: a greener chemical approach for the synthesis of biologically active 3,4-dihydropyrimidin-2(1H)-ones/thiones. In: Brahmachari G., editor. *Green synthetic approaches for biologically relevant heterocycles*. 1st ed. Elsevier Science Publishing Co. Inc.; pp. 317, **2015**.
- NOOR A., MUSHTAQ W., QADIR I., MASOODI M.H. Biological activities of dihydropyrimidinones. In *Dihydropyrimidinones as Potent Anticancer Agents, Medicinal Chemistry Perspective*. Elsevier Science Publishing Co. Inc.; pp. 39, **2023**.
- ZARENEZHAD E., FARJAM M., IRAJI A. Synthesis and biological activity of pyrimidines-containing hybrids: Focusing on pharmacological application. *Journal of Molecular Structure*, **1230**, 129833, **2021**.
- SÁNCHEZ-SANCHO F., ESCOLANO M., GAVIÑA D., CSÁKY A.G., SÁNCHEZ-ROSELLÓ M., DÍAZ-OLTRA S., DEL POZO C. Synthesis of 3, 4-dihydropyrimidin (thio) one containing scaffold: Biginelli-like reactions. *Pharmaceuticals*, **15** (8), 948, **2022**.
- BRANDAO P., MARQUES C., BURKE A.J., PINEIRO M. The application of isatin-based multicomponent-reactions in the quest for new bioactive and druglike molecules. *European Journal of Medicinal Chemistry*, **211**, 113102, **2021**.
- DESAI N.C., TRIVEDI A.R., VAGHANI H.V., SOMANI H.C., BHATT K.A. Synthesis and biological evaluation of 1, 3, 4-oxadiazole bearing dihydropyrimidines as potential antitubercular agents. *Medicinal Chemistry Research*, **25**, 329, **2016**.
- KAZEMI M., SHIRI L., KOHZADI H. Synthesis of pyrano [2, 3, d] pyrimidines under green chemistry. *Journal of Materials and Environmental Science*, **8** (9), 3410, **2017**.
- SONAWANE R.P. Green synthesis of pyrimidine derivative. *International Letters of Chemistry, Physics and Astronomy*, **2**, 64, **2014**.
- LEE J., KIM S.M., LEE I.S. Functionalization of hollow nanoparticles for nanoreactor applications. *Nano Today*, **9** (5), 631, **2014**.
- HU P., MORABITO J.V., TSUNG C.K. Core-shell catalysts of metal nanoparticle core and metal-organic framework shell. *ACS Catalysis*, **4** (12), 4409, **2014**.
- SONI J., SAHIBA N., SETHIYA A., AGARWAL S. Polyethylene glycol: A promising approach for sustainable organic synthesis. *Journal of Molecular Liquids*, **315**, 113766, **2020**.
- HOFFMANN M.M. Polyethylene glycol as a green chemical solvent. *Current Opinion in Colloid & Interface Science*, **57**, 101537, **2022**.
- SEEBACH D. Organic synthesis—where now? *Angewandte Chemie International Edition in English*, **29** (11), 1320, **1990**.
- WHITESIDES G.M., WONG C.H. Enzymes as catalysts in synthetic organic chemistry [new synthetic methods (53)]. *Angewandte Chemie International Edition in English*, **24** (8), 617, **1985**.
- EKEZIE F.G.C., SUN D.W., HAN Z., CHENG J.H. Microwave-assisted food processing technologies for enhancing product quality and process efficiency: A review of recent developments. *Trends in Food Science & Technology*, **67**, 58, **2017**.
- LEONELLI C., MASON T.J. Microwave and ultrasonic processing: Now a realistic option for industry. *Chemical Engineering and Processing: Process Intensification*, **49** (9), 885, **2010**.
- MARIDEVARMATH C.V., NAIK L., NEGALURMATH V.S., BASANAGOUDA M., MALIMATH G.H. Synthesis, characterization and photophysical studies on novel benzofuran-3-acetic acid hydrazide derivatives by solvatochromic and computational methods. *Journal of Molecular Structure*, **1188**, 142, **2019**.
- MARIDEVARMATH C.V., NAIK L., NEGALURMATH V.S., BASANAGOUDA M., MALIMATH G.H. Synthesis, photophysical, DFT and solvent effect studies on biologically active benzofuran derivative:(5-methyl-benzofuran-3-yl)-acetic acid hydrazide. *Chemical Data Collections*, **21**, 100221, **2019**.
- THIPPESWAMY M.S., NAIK L., MARIDEVARMATH C.V., SAVANUR H.M., MALIMATH G.H. Studies on the characterisation of thiophene substituted 1, 3, 4-oxadiazole derivative for the highly selective and sensitive detection of picric acid. *Journal of Molecular Structure*, **1264**, 133274, **2022**.

25. ALI A.M.E.S., EL MAGHRABY G.M., ABDELAZIZ A.E., SOLIMAN A.M., SAIED E.M., MAZYED E.A. Co-processing of fluconazole with menthol for enhanced dissolution and anti-fungal activity: Preparation of orodispersable tablets. *Journal of Drug Delivery Science and Technology*, **88**, 104937, **2023**.
26. POWDER-GEORGE Y.L. *Terpenoids, Pharmacognosy (Second Edition), Fundamentals, Applications, and Strategies*, Elsevier Science Publishing Co. Inc., pp. 253, **2024**.

Supplementary Material

Supplementary material can be obtained online

<https://www.pjoes.com/SuppFile/183851/9181/6bd81b8711bda5e1e6127350596e823d/>